06,13,16

Local distortions of the perovskite structure in high-temperature Raman spectra of the relaxor ferroelectric $PbMg_{1/3}Nb_{2/3}O_3$

© N.K. Derets[1], R.S. Katiyar[2], J.-H. Ko[3], S.G. Lushnikov[1,¶]

[1] Ioffe Institute,
St. Petersburg, Russia
[2] Department of Physics, University of Puerto Rico,
San Juan, Puerto Rico, USA
[3] School of Nano Convergence Technology,
Nano Convergence Technology Center, Hallym University,
Gangwondo, Korea

¶ E-mail: sergey.lushnikov@mail.ioffe.ru

Received July 25, 2025
Revised July 26, 2025
Accepted July 27, 2025

In this paper, we present the results of a study of the optical phonon behavior of the $PbMg_{1/3}Nb_{2/3}O_3$ (PMN) crystal using Raman scattering in the temperature range from 1100 to 300 K. At $T > 1050$ K, polarized „weak" modes and a quasi-elastic scattering component are observed in the Raman spectra of PMN. These „weak" modes can be associated with local distortions of the crystal lattice caused by disorder in the B-sublattice of the perovskite structure. When cooling PMN, in the vicinity of $T_1 \approx 1050$ K, the intensity of the observed modes in the Raman spectrum increases abruptly by more than an order of magnitude, the frequencies of these modes do not demonstrate visible anomalies. Further cooling of the PMN crystal leads to the restoration of the polarized Raman spectrum, well known from the literature. In the temperature evolution of the main modes, the Burns temperature ($T_d \approx 640$ K) can be distinguished, in the vicinity of which the intensities of the modes in the scattering spectra with VV polarization begin to increase linearly with decreasing temperature, in the absence of anomalies in the frequency behavior. Anomalies in the temperature dependences of the optical phonon frequencies are observed in the vicinity of $T^* \approx 400$ K, where a change in the short-range order dynamics is assumed. The results obtained are discussed within the framework of modern physics of relaxor ferroelectrics.

Keywords: ferroelectrics, lattice dynamics, Raman scattering, optical phonons.

DOI: 10.61011/PSS.2025.08.62270.215-25

1. Introduction

Lead magnesium niobate crystals belong to a large group of partially disordered perovskites of a general formula $AB_{1-x}B'_xO_3$, in which a wide spectrum of various physical states is observed (ferroelectric, ferroelastic, antiferromagnetic, etc.) [1]. Intense studies of the structure and the physical properties made it possible to distinguish a family of relaxor ferroelectrics (relaxors) [2], which are characterized by a wide, frequency-dependent anomaly of a dielectric response, which is generally unrelated to a structural phase transition. A high number of experimental and theoretical studies has not resulted in consensus in discussing the mechanisms of origin of unique dielectric and piezoelectric properties of the relaxors, but shown a key role of the short-range order in dynamics of the crystal lattices of the disordered perovskites [1,3–6].

$PbMg_{1/3}Nb_{2/3}O_3$ (PMN) is a model example of the relaxor ferroelectric. It has been intensely scrutinized for the last 60 years, thereby making it possible to consider it as the most studied relaxor [1–6], while gigantic values of piezoelectric and dielectric magnitudes of the electromechanical responds of solid solutions based thereon [7] have been applied for a long time when creating basic elements of sonars, sensors, actuators and other devices. A macroscopic cubic symmetry (the space group $Pm\bar{3}m$) is preserved in PMN within the entire studied temperature range from the helium to high ones [8], while the maximum of permittivity (T_m) at 10 kHz is observed around 273 K [1]. It is assumed today that the anomaly of ε' observed at T_m is contributed both by soft optical phonons as well as polar nanoregions (PNR) that originate around $T_d \approx 640$ K [3,6]. The dynamics of the PNRs and their relation to a phonon subsystem of the relaxors is widely discussed in the literature [3–6]. It is found that the decrease of the temperature results in change of the behavior of PNR dynamics and the emergence of static PNRs with the R3c symmetry around $T^* \approx 400$ K [9]. The PNRs are finally „frozen" around the Vogel–Fulcher temperature $T_{VF} \approx 225$ K, thereby resulting in the emergence of a nonergodic relaxor state [1,3].

Polarized spectra of Raman light scattering were observed in the PMN for the first time in the study [10]. Existence of the mutually similar polarized Raman spectra in relaxors with perovskite structure, which are forbidden by selection rules for the $Pm\bar{3}m$ symmetry, is still being discussed. Here, we specify two basic representations of the nature of the emergence of Raman scattering in these compounds. The first one was proposed by Burns and Scott [11]. From their point of view, based on a predominant role of disordering, lines appear in the PMN Raman scattering spectrum due to a loss of both translational and inversion symmetry, which is caused by disorder in the B-sublattice. The second approach involves taking into account „a symmetry" of oscillations of the relaxors that are active in the Raman scattering spectra [12–14]. According to this point of view, it is assumed that ordering occurs at crystal regions with a ratio of 1 : 1 between the cations B' and B'', thereby resulting in formation of a lattice cell of „superstructure" with the $Fm\bar{3}m$ symmetry. This consideration is also suitable, if the complex perovskite consists of nanoregions with the $Fm\bar{3}m$ symmetry, which have quite a big size for creating conditions for the emergence of Raman scattering. No superlattice reflections in data of X-ray diffraction and neutrongraphic analysis [8] as well as existence of the polarized Raman spectra at the temperatures above the area of the emergence of the polar nanoregions [4,14] makes it difficult to use a „symmetry" approach for explaining existence of the Raman spectra in the relaxors with the ratio of 1 : 2 between the cations B' and B''. Further development of existing or new representations requires detailed temperature studies, especially, in the high-temperature range. The first papers of the high-temperature Raman studies of the relaxors with perovskite structure $PbMg_{1/3}Ta_{2/3}O_3$ (PMT) and $PbSc_{1/2}Ta_{1/2}O_3$ (PST) reported disappearance of the polarized Raman spectra when $T > 950$ K and related it to a dynamic phase transition from $Fm\bar{3}m$ into $Pm\bar{3}m$, at which non-equivalence of oxygen octahedra, responsible for appearance of four active Raman modes, vanished [12]. The same model was later used when discussing disappearance of the Raman spectra in the relaxors $PbIn_{1/2}Nb_{1/2}O_3$ [15], PMN [16] and in a low-k-dielectric $BaMg_{1/3}Ta_{2/3}O_3$ [17], but high-temperature evolution of the Raman spectra in the relaxors was not studied in detail. It motivated us to investigate high-temperature ($T > 900$ K) dynamics of the crystal lattice in the model PMN relaxor using Raman scattering.

2. Materials and methods

Raman scattering was measured in a backscattering geometry using a Jobin-Yvon T64000 spectrometer. Radiation of an argon laser Innova 99 with the wavelength of 514.5 nm was focused on a sample into a region of the diameter of below 2 μm by means of an optical polarization microscope. A spectrum integration time, a gap width and a laser beam power were corrected in order to provide a high signal/noise ratio. Typical spectrum resolution for the Raman scattering system with the 1800 line/mm grid and the 1-inch CCD matrix (the charge-coupling device) was below 1 cm^{-1}. The system was calibrated by the Si spectra at the room temperature. For high-temperature measurements, the sample was placed in an optical heating chamber Linkam TS1500. The temperature maintenance accuracy was ± 1 K. The samples were prepared by using the PMN crystals grown by the Czochralski method (boules). A PMN plate cut out of the boule along main crystallographic directions was polished to optical quality and had the sizes $1 \times 2 \times 3$ mm. The wave vector of the phonon was directed along $\langle 001 \rangle$, while polarization of incident light was parallel to $\langle 010 \rangle$.

Analysis of the experimental light scattering spectra included use of a sum of the Lorentz function for the phonons and the expression for the Debye relaxor, which described quasielastic light scattering:

$$I_0(v) = I_b + \frac{2A_{QELS}}{\pi} \cdot \frac{\Gamma_{QELS}}{4v^2 + \Gamma_{QELS}^2} + \sum_i \frac{2A_i}{\pi} \cdot \frac{\Gamma_i}{4(v - v_i)^2 + \Gamma_i^2}, \quad (1)$$

where A_i — the intensity of, v_i — the position of the lines in the spectrum, Γ_i — full width at half maximum for the line in the spectrum, I_b — the background intensity, A_{QELS} — the intensity of and Γ_{QELS} — full width at half maximum of quasielastic light scattering, respectively. When fitting the experimental PMN Raman scattering spectra, the intensity of the line (I) was corrected with taking into account the Bose-Einstein coefficient by using the expression (2):

$$I(v) = I_0(v)\left\{\left[\exp\left(\frac{hv}{k_B T}\right) - 1\right]^{-1} + 1\right\}, \quad (2)$$

Here, h — the Planck constant, k_B — the Boltzmann constant and T — the sample temperature. The spectra were processed using the least-square method in the MATLAB software. It should be noted that a function of the damped harmonic oscillator (DHO) is often used in the processing of the experimental spectra of Raman scattering in the crystals. The study [18] exemplifies processing of the PMN spectra using the DHO function as well as compares the obtained results with calculations using the Lorentz functions. It was found that there were small differences in the temperature dependences obtained when processing the experimental spectra by means of the Lorentz and DHO functions. For this reason, in the present calculations we used the Lorentz function when processing the experimental scattering spectra. An additional argument in favor of this model of spectrum processing is an anomalously large width of the discussed modes, which may indicate the contribution to Raman scattering by phonons from other points of the Brillouin zone. Results of the studies of quasielastic light scattering in the PMN Raman scattering spectra will be published separately.

3. Results and discussion

Figure 1, *a* and *c* shows the examples of processing of (when $T = 373$ K) and the temperature evolution of (Figure 1, *b* and *d*) the PMN Raman spectra in vertical-vertical polarization (VV) and vertical-horizontal (VH) polarization. The experimental spectra with VH-polarization exhibit two components (A and B) of a split mode with the frequencies $\nu_B \approx 41\,\text{cm}^{-1}$ and $\nu_A \approx 57\text{cm}^{-1}$ (Figure 1, *b*). Two main lines can be seen in the VV-polarization: the low-frequency mode (C) with the frequency $\nu_C \approx 48.5\,\text{cm}^{-1}$ and the high-frequency (D-mode), with the frequency $\nu_D \approx 787\,\text{cm}^{-1}$ (Figure 1, *d*). The Raman scattering spectra obtained during our measurements are in a good agreement with the previously published ones [14,16,18]. In the present study, we will discuss the temperature behavior of the four above-said main modes. It is well seen in Figure 1, *b* and *d* that the intensity of the spectra varies with an increase of the temperature and then starts decreasing around 950 K. Further increase of the temperature results in disappearance of the intense Raman spectrum in PMN when $T > 1050$ K (see Figure 1, *b* and *d*). The spectra and their temperature variations, which are shown in Figure 1, are in good agreement with the previously published ones [16,18]. Analysis of the experimental scattering spectra around 1050 K and higher (Figure 2) has shown that the situation is more complex than it was previously believed to be [16]. Indeed, the intensity of the spectra decreased abruptly by more than an order of magnitude around $T_1 \approx 1050$ K. But, nevertheless, we observe weak lines instead of the intense ones that were visible at the low temperatures (Figure 2). When $T > 1050$ K, we see modes C and D in VV-polarization and two modes A and B in VH-polarization.

Quasielastic scattering is also preserved in the low-frequency range of the Raman spectra when $T > 1050$ K (see Figure 2). Additional specific features of the spectrum, which are observed at the low temperatures, almost disappear except for the spectrum range from 250 to 400 cm^{-1}, which becomes nonpolarized and is observed in both the polarizations (see Figure 2). It should be noted that the temperature changes of the spectrum at $T_1 \approx 1050$ K are reversible: decrease of the temperature results in reappearance of the initial PMN Raman spectrum.

Thus, the evolution of the Raman scattering spectra in PMN observed by us significantly differs from the literature data [16]. It can be related to a progress in the physical experiment technique (including when measuring the temperatures), which made it possible to perform the high-temperature measurements with high accuracy in a data accumulation mode. The weak Raman scattering spectra in PMN, which are shown in Figure 2, can be explained by assuming the existence of weak distortions of the perovskite structure. Unfortunately, the literature has no data on studying the PMN structure when $T > 1023$ K. The results of X-ray diffraction measurements of PMN, which are known to us, are completed at 1023 K. It follows

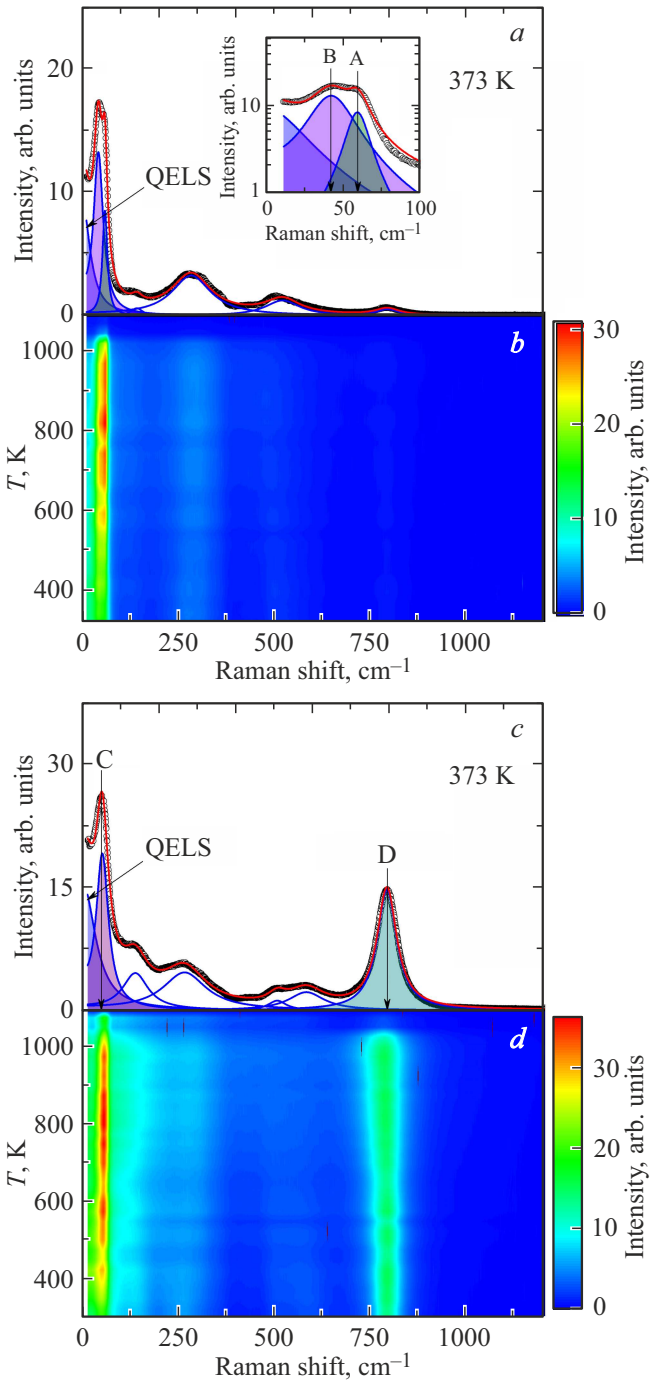

Figure 1. Examples of the PMN Raman spectra when $T = 373$ K (with processing, see the text) and their temperature evolution: *a* and *b* — VH-polarization; *c* and *d* — VV-polarization. QELS — the contribution by quasielastic light scattering. The Figures *a* and *c* show the results of data fitting (the red line) using the equations (1) and (2). The experimental data is shown by black circles.

from them that in the high-temperature range the lead ions are in Wyckoff perovskite positions, while distortions of the structure are determined by statistic distribution (1 : 2) Mg^{2+} and Nb^{5+} in the B-sublattice of the crystal. Thus, the

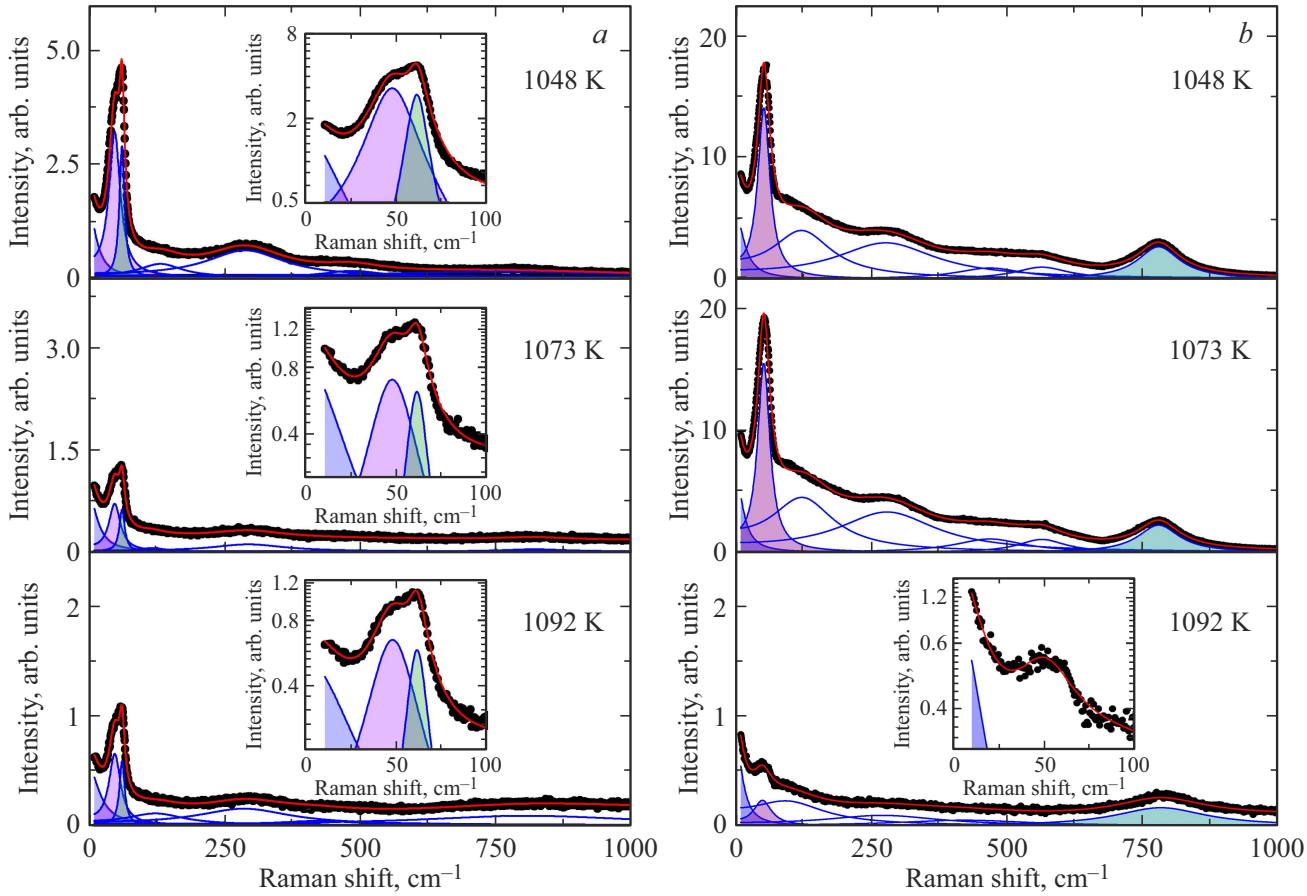

Figure 2. Experimental PMN Raman spectra in the high-temperature range: *a*) VH-polarization, *b*) VV-polarization. They include the results of data fitting (the red line) using the equations (1) and (2). The experimental data is shown by black circles.

PMN structure has two types of the nonequivalent oxygen octahedrons, whose center includes Mg or Nb with different ionic radii [8]. Statistic distribution of these nonequivalent oxygen octahedrons across the crystal volume results in local distortions of the perovskite structure, which can be responsible for appearance of the weak lines in Raman scattering in PMN when $T > 1050$ K. The decrease of the temperature results in displacement of the lead ions along the direction of the type $\langle 111 \rangle$ and/or $\langle 110 \rangle$, an increase of distortions of the PMN crystal lattice and, apparently, an increase of the intensity of the Raman spectra. Similar correlation in the behavior of lead with simultaneous increase of the intensity of the modes in the Raman spectra was discussed in the study [19] and observed in the PMT crystals with variation of the temperature [20]. Further cooling of the PMN crystal results in formation of the dynamic polar nanoregions that are based on local distortions of the perovskite structure [3–6].

Now let us consider the temperature dependences of the frequency, full width at half maximum (FWHM) and the intensity of the considered main modes obtained during fitting of the experimental data using the equations (1) and (2), which are shown in Figures 3 and 4. The temperature behavior of the two modes (A and B) in VH-polarization of the PMN Raman spectra is shown in Figure 3. It is well seen that the intensities of the both modes monotonically decrease when heating the crystal up to the temperatures of 1000 K (Figure 3). Further increase of the temperature results in a jump-like decrease of the intensity of the modes A and B by almost 2 times around $T_1 \approx 1050$ K, while at the same time the frequencies of the respective modes demonstrate weak „kinks“ in the temperature dependences $\nu_A(T)$ and $\nu_B(T)$ (Figure 3). The weak „kinks“ can be related to an increase of the error in the high-temperature measurements and calculations.

Analyzing the temperature behavior of the frequencies of the modes A and B, it is worth noting that the modes are „softening“, increasing in the width with the temperature decrease (Figure 3). In doing so, no anomalies are detected in the temperature behavior of the modes around T_d. The differences in the behavior of the frequencies of the modes A and B are observed around T^*, where the mode A stops „softening“, whereas the frequency of the mode B continues its decrease with cooling of the crystal (Figure 3). This behavior of the modes A and B differs from what is published in the paper [18], in which the anomalies are observed around T_d.

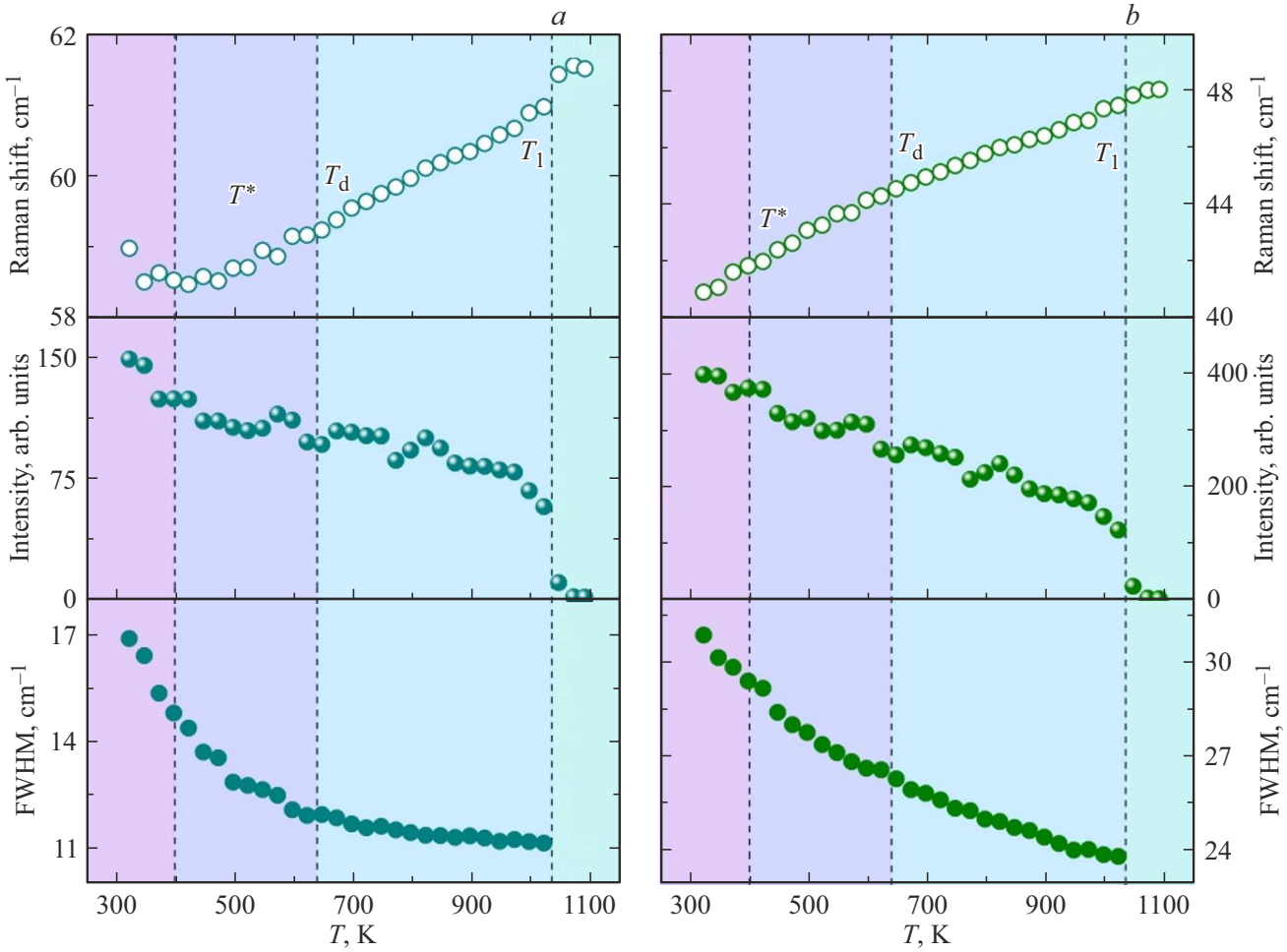

Figure 3. Temperature dependences of the frequency, the intensity and full width at half maximum (FWHM) for the modes *a*) A and *b*) B in the PMN Raman spectra with VH-polarization.

The temperature behavior of the modes C and D in the PMN Raman spectra with VV-polarization is shown in Figure 4. The low-frequency mode C (Figure 4, *a*) around T_1 significantly changes the intensity and demonstrates a slight kink in the frequency behavior. With reduction of the temperature around T_d the temperature dependence of the intensity of the mode C changes its behavior, abruptly increasing with the temperature decrease. The frequency of this mode is „softening“ when the PMN is cooled, but it becomes temperature-independent around T^*. The changes in the behavior of the mode C, which are observed by us, differ from the one presented in the study [18]. No anomalies are observed in the behavior of the width of the mode C with variation of the temperature.

The temperature behavior of the high-frequency mode D (Figure 4, *b*) fundamentally differs from the observed behavior of the low-frequency modes A, B and C. It is well seen in Figure 4 that when the PMN crystal is heated the frequency of the mode D decreases, while its width increases, in the same way as in case of the isostructural crystals $PbNi_{1/3}Nb_{2/3}O_3$ — PNN and $PbCo_{1/3}Nb_{2/3}O_3$ — PCN [21,22]. Around T_1, the intensity of the mode D decreases by a jump by more than an order to the values that do not make it possible to correctly determine (with a low error) values of the frequency and the half-width when $T > 1050$ K (see Figure 2). Decrease of the temperature demonstrates an anomaly in the dependence $I_D(T)$ around T_d, below which we observe a linear increase of the intensity of the mode D. Anomalies in the behavior of the intensities of the modes C and D around T_d seem to be related to formation of the polar nanoregions. The behavior of the main phonon lines, which has been considered by us, has the same tendency as in the study [18], while the noted differences can be related both to the different experimental geometry (the 180-degree scattering geometry in the present study and the 90-degree geometry in the study [18]) and differences in the methods of scattering spectra processing.

By summing the changes observed by us in the behavior of the main modes of the PMN-crystal Raman spectra during cooling, it is necessary to note no visible anomalies in the temperature dependence of the frequencies and the widths, with pronounced changes in the temperature

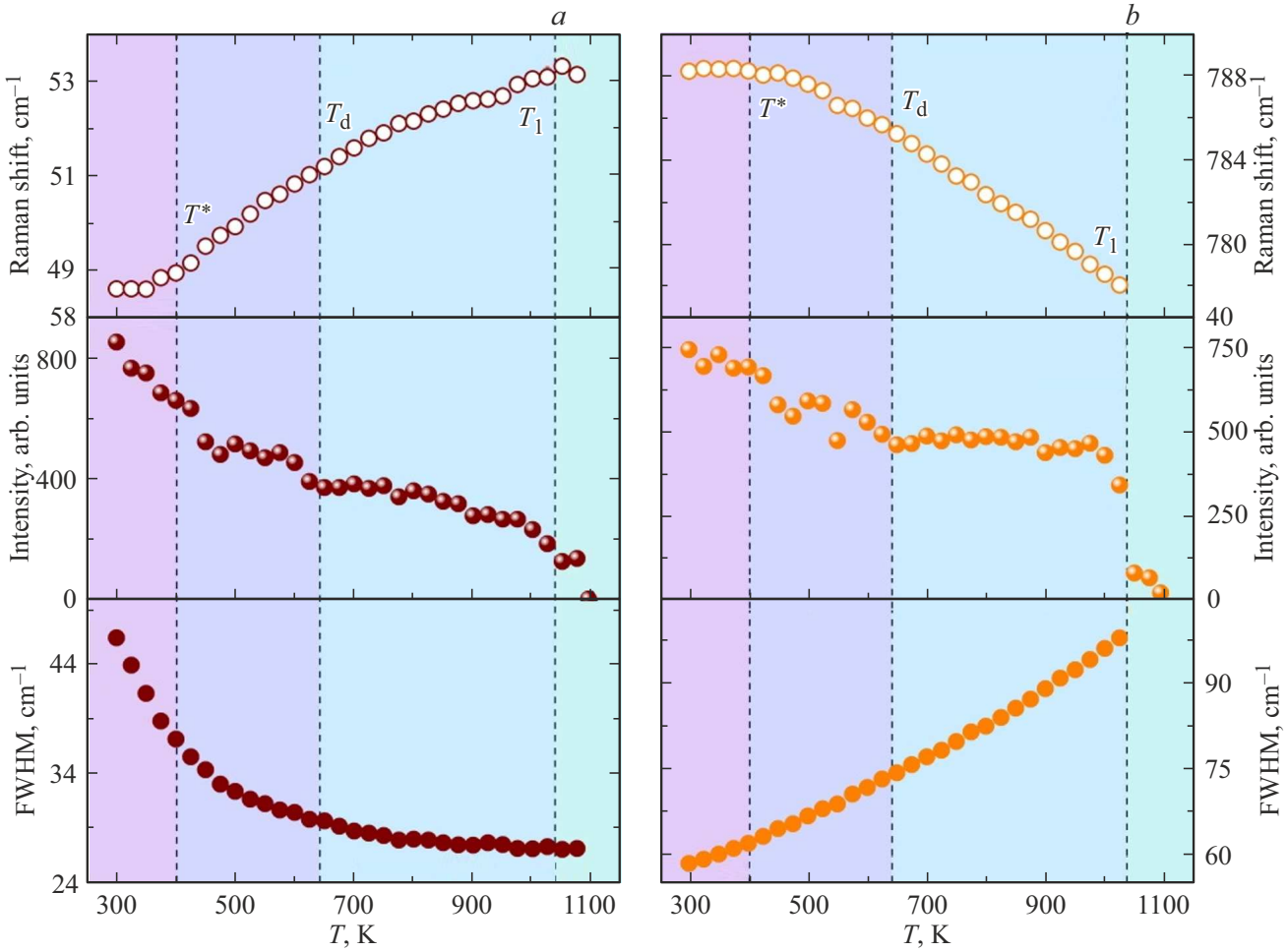

Figure 4. Temperature dependences of the frequency, the intensity and full width at half maximum (FWHM) for the modes *a*) C and *b*) D in the PMN Raman spectra with VV-polarization.

evolution of the intensity. It is another argument in favor of the assumption about a decisive role of the short-range order dynamics (local distortions, polar nanoregions, etc.) in the behavior of the Raman spectra in PMN.

4. Conclusion

The high-temperature dynamics of the lattice in the PMN crystals was studied using Raman scattering within the temperature range from 1100 to 300 K. The performed measurements were the first to show existence of the polarized weak modes in the light structure modes, which were related to local distortions of the perovskite structure at the temperatures above 1050 K. These local distortions occur as a result of a disorder in the perovskite B-sublattice due to statistical distribution 1 : 2 of the ions Mg^{2+} and Nb^{5+}. We have found the jump-like decrease (by more than an order) of the intensity of the observed main lines, with the weak anomalies in the temperature dependences of the frequencies around $T_1 \approx 1050$ K. Further decrease of the temperature showed the anomalous behavior of the intensity of the modes in the VV-polarized Raman spectra in the neighborhood of formation of the polar nanoregions ($T_d \approx 640$ K) without anomalies of the frequencies and widths of the discussed modes. We observe the increase of the intensity of the modes in VH-polarization when $T < 1050$ K within the entire temperature range. This behavior of the intensities of the main modes can be related to the increase of displacement of the lead ions along the selected directions of the type ⟨111⟩ and/or ⟨110⟩ from the Wyckoff positions when the PMN crystal is cooled [8]. The issue of the mechanisms of the abrupt increase of the intensities of the lines in the PMN Raman spectra around $T_1 = 1050$ K is still open. Further studies of the structure and dynamics of the crystal lattice of the relaxor ferroelectrics within the high temperatures are required.

Funding

This study was financed under the state assignment of the Ministry of Education and Science of the Russian Federation FFUG-2024-0042.

Conflict of interest

The authors declare that they have no conflict of interest.

References

[1] G.A. Smolensky, V.A. Bokov, V.A. Isupov, N.N. Krainik, R.E. Pasynkov, A.I. Sokolov, N.K. Yushin. Ferroelectrics and Related Materials. Gordon & Breach, N.Y. (1984). 421 p.
[2] L.E. Cross. Ferroelectrics **76**, *1*, 241 (1987).
[3] A.A. Bokov, Z.-G. Ye. J. Mater. Sci. **41**, *1*, 31 (2006).
[4] R.A. Cowley, S.N. Gvasaliya, S.G. Lushnikov, B. Roessli, G.M. Rotaru. Adv. Phys. **60**, *2*, 229 (2011).
[5] M.E. Manley. In: Frustrated Materials and Ferroic Glasses. Springer Series in Materials Science, v. 275 / Eds T. Lookman, X. Ren. Springer, Cham, Switzerland (2018). P. 101.
[6] S. Kamba. APL Mater. **9**, *2*, 020704 (2021).
[7] S.-E. Park, T.R. Shrout. J. Appl. Phys. **82**, *4*, 1804 (1997).
[8] P. Bonneau, P. Gamier, G. Calvarin, E. Husson, J.R. Gavarri, A.W. Hewat, A. Morell. J. Solid State Chem. **91**, *2*, 350 (1991).
[9] B. Dkhil, P. Gemeiner, A. Al-Barakaty, L. Bellaiche, E. Dul'kin, E. Mojaev, M. Roth. Phys. Rev. B **80**, *6*, 064103 (2009).
[10] G.A. Smolensky, I.G. Siny, R.V. Pisarev, E.G. Kuzminov. Ferroelectrics **12**, *1*, 135 (1976).
[11] G. Burns, B.A. Scott. Solid State Commun. **13**, *3*, 423 (1973).
[12] I.G. Siny, T.A. Smirnova. Ferroelectrics **90**, *1*, 191 (1989).
[13] I.G. Siny, R.S. Katiyar, A.S. Bhalla. J. Raman Spectr. **29**, *5*, 385 (1998).
[14] I.G. Siny, R.S. Katiyar, A.S. Bhalla. Ferroelectrics Rev. **2**, *1–2*, 51 (2000).
[15] A. Kania, K. Roleder, G.E. Kugel, M. Hafid. Ferroelectrics **135**, *1*, 75 (1992).
[16] I.G. Siny, S.G. Lushnikov, R.S. Katiyar, V.H. Schmidt. Ferroelectrics **226**, *1*, 191 (1999).
[17] I.G. Siny, R. Tao, R.S. Katiyar, R. Guo, A.S. Bhalla. J. Phys. Chem. Sol. **59**, *2*, 181 (1998).
[18] O. Svitelskiy, J. Toulouse, G. Yong, Z.-G. Ye. Phys. Rev. B **68**, *10*, 104107 (2003).
[19] T. Egami, E. Mamontov, W. Dmowski, S.B. Vakhrushev. AIP Conf. Proceed. **677**, *1*, 48 (2003).
[20] S.G. Lushnikov, S.N. Gvasaliya, R. Katiyar. Phys. Rev. B **70**, *17*, 172101 (2004).
[21] N.K. Derets, A.I. Fedoseev, T.A. Smirnova, J.-H. Ko, S.G. Lushnikov. JETP Lett. **120**, *10*, 741 (2024).
[22] N.K. Derets, A.I. Fedoseev, Dzh.-Kh. Ko, S.G. Lushnikov. Pis'ma v ZhETF **121**, *12*, 952 (2025). (in Russian).

Translated by M.Shevelev